

MRI of the Pituitary Gland

Jean-François Bonneville
Fabrice Bonneville
Françoise Cattin
Sonia Nagi

MRI of the Pituitary Gland

Jean-François Bonneville
Fabrice Bonneville
Françoise Cattin
Sonia Nagi

MRI of the Pituitary Gland

With a Foreword by A. Beckers

 Springer

Jean-François Bonneville, MD
Department of Endocrinology
CHU Sart-Tilman
Liège
Belgium

Fabrice Bonneville, MD, PhD
Department of Neuroradiology
University Hospital Paul Sabatier
Toulouse
France

Françoise Cattin, MD
Department of Neuroradiology
and Endovascular Therapy
University Hospital of Besançon
Besançon
France

Sonia Nagi, MD
Faculty of Medicine
National Institute of Neurology
University of Tunis El Manar
Tunis
Tunisia

ISBN 978-3-319-29041-6 ISBN 978-3-319-29043-0 (eBook)
DOI 10.1007/978-3-319-29043-0

Library of Congress Control Number: 2016935498

© Springer International Publishing Switzerland 2016

This work is subject to copyright. All rights are reserved by the Publisher, whether the whole or part of the material is concerned, specifically the rights of translation, reprinting, reuse of illustrations, recitation, broadcasting, reproduction on microfilms or in any other physical way, and transmission or information storage and retrieval, electronic adaptation, computer software, or by similar or dissimilar methodology now known or hereafter developed.

The use of general descriptive names, registered names, trademarks, service marks, etc. in this publication does not imply, even in the absence of a specific statement, that such names are exempt from the relevant protective laws and regulations and therefore free for general use.

The publisher, the authors and the editors are safe to assume that the advice and information in this book are believed to be true and accurate at the date of publication. Neither the publisher nor the authors or the editors give a warranty, express or implied, with respect to the material contained herein or for any errors or omissions that may have been made.

Printed on acid-free paper

This Springer imprint is published by Springer Nature
The registered company is Springer International Publishing AG Switzerland

Foreword

The pituitary is a tiny and fascinating gland of extreme importance biologically, surrounded by an array of vital structures. Correct decision-making about the pituitary is of the utmost clinical importance. While we can infer pathology from hormonal profiles and clinical symptoms, neuroradiological images often provide us with the key information in planning correct treatment. Thankfully, this potentially confusing experience for the uninitiated is made far easier with the publication of *MRI of the Pituitary Gland* by Prof. Jean-Francois Bonneville and his co-authors. This new book is aimed at an audience far wider than just neuroradiologists, although they too will find much of interest therein. It is for all of us, particularly endocrinologists, who find ourselves faced regularly with clinical problems that may be related to pituitary pathology. The book covers all of the major topics of importance, building from the foundations of normal appearance and characteristics of the pituitary and surrounding structures to cover tumors and related disorders. It is remarkable how many differential diagnoses must be entertained when assessing disorders of pituitary appearance on MRI. The pituitary gland is not only the site of primary pathologies but also can act as an important site of secondary systemic pathology of immune, inflammatory, or infectious diseases. Prof. Bonneville guides us through these various possibilities and carefully shows us how they may be distinguished from one another. Furthermore, he integrates his long experience as a diagnostician and researcher by adding information on how the appearance of pituitary tumors can determine aspects of their clinical behavior (e.g., acromegaly). Prof. Bonneville is an acknowledged world-leading authority in neuroradiology of the pituitary and surrounding structures who gained this experience through a lifetime of clinical and teaching work in France. Since he retired from his hospital position in France, happily he has agreed to continue sharing his experience with us having swapped the Jura for the Ardennes of Belgium. So I have now had the personal pleasure of benefiting from his input on clinical neuroradiology on my own patients and undertaking new research working together as colleagues in Liège. I was delighted on many occasions to attend lectures and courses given by Prof. Bonneville on the topic of pituitary neuroradiology. These events never fail to be informative and interesting, given his wide breadth of knowledge and experience. However, these are not entirely relaxed encounters, as Prof. Bonneville always ends with a quiz on what he has just been teaching and illustrating. I have often seen quite experienced senior endocrinologists

squirming under questioning when interpreting pituitary imaging! This is, for me, one of the important reasons why this book is so welcome. Pituitary neuroradiology is complex and there are many pitfalls of which we can become victims. With this book we can learn to identify those elements that can confound correct interpretations, and with the copious illustrations and images we can visualize the pathology clearly and memorably.

Albert Beckers MD, PhD
Chief, Department of Endocrinology
Centre Hospitalier Universitaire de Liège
University of Liège, Liège, Belgium

Preface

Magnetic resonance imaging (MRI) is currently considered as a major keystone of the diagnosis of diseases of the hypothalamic-hypophyseal region. However, the relatively small size of the pituitary gland, its deep location at the skull base, and the numerous physiological variants present in this area impede the precise assessment of the anatomical structures and, particularly, of the pituitary gland itself.

The diagnosis of the often tiny lesions of this region, such as pituitary microadenomas, is thus difficult if the MRI technology is not optimized and if potential artifacts and traps are not recognized. Advanced MRI technology is able not only to depict small lesions with greater reliability, but also helps in the differential diagnosis of large tumors, particularly for which defining the presence or absence of invasion of the cavernous sinus is an important task.

This book describes and illustrates the role of MRI in the diagnosis of the different lesions of the sellar region, from the common prolactinoma, to the nonfunctioning adenoma and the Rathke cleft cyst, to the less frequent lymphocytic hypophysitis or pituitary corticotroph adenoma in Cushing disease, and other neoplastic and non-neoplastic entities.

Finally, the book emphasizes the necessity of adapting the MRI sequences to the symptoms of each particular patient and of working in close collaboration with all specialists involved in the pathology of the sellar area.

Jean-François Bonneville
Fabrice Bonneville
Françoise Cattin
Sonia Nagi

Contents

1 MRI Technique and Radiological Anatomy of the Pituitary Gland	1
1.1 Basic MRI Sequences	1
1.2 Additional Sequences	1
1.3 Advanced MRI Techniques	2
1.4 Radiological Anatomy	2
1.4.1 The Anterior Lobe of the Pituitary Gland	2
1.4.2 The Pituitary Stalk	6
1.4.3 The Posterior Lobe of the Pituitary Gland	6
1.4.4 The Cavernous Sinus	7
2 Traps and Artifacts	13
3 Small Sella and Convex Pituitary Gland	19
4 Nonfunctioning Pituitary Macroadenoma: General Points	25
5 Prolactinoma in Women	35
6 Prolactinoma and Dopamine Agonists	45
7 Normal Pituitary Gland and Pregnancy	53
8 Pituitary Tumors and Pregnancy	57
9 Prolactinoma in Men	65
10 Aggressive Pituitary Adenoma	71
11 Cavernous Sinus Invasion	77
12 Hemorrhagic Pituitary Adenoma	83
13 Pituitary Apoplexy	89
14 Acromegaly	97
15 Cushing Disease	107
16 Silent Corticotroph Pituitary Adenoma	113
17 Pituitary Carcinoma	117
18 Ectopic Pituitary Adenoma	121
19 Rathke Cleft Cyst: Asymptomatic	125

20	Rathke Cleft Cyst: Symptomatic and Complicated	135
21	Pituitary Adenoma and Concomitant Sellar Lesions	145
22	Craniopharyngioma	153
23	Pre- and Suprasellar Meningiomas	165
24	Cavernous Sinus Meningioma	173
25	Intraoperative MRI	179
26	The Early Postoperative Sella	183
27	The Late Postoperative Sella	189
28	Complications of Pituitary Surgery	197
29	The Pituitary Gland After Radiation Therapy	205
30	Chiasmatic and Hypothalamic Gliomas	211
31	Suprasellar Germinoma	217
32	Melanoma	225
33	Pituitary Metastases	229
34	Sellar and Suprasellar Lymphoma	235
35	Cavernous Sinus Lesions	241
35.1	Aneurysm	241
35.2	Cavernous Hemangioma	243
35.3	Cavernous Sinus Thrombosis	243
35.4	Tolosa-Hunt Syndrome	248
35.5	Trigeminal Schwannoma	249
35.6	ENT Lesions	249
35.7	Metastases	251
36	Primary Neurohypophyseal Glial Tumors	257
37	Chordoma and Chondroma/Chondrosarcoma	261
38	Hamartoma of the Tuber Cinereum	271
39	Sphenoid Mucocele	277
40	Primary Hypophysitis	283
41	Pituitary in Systemic Diseases	293
41.1	Sarcoidosis	293
41.2	Histiocytosis	296
41.3	Wegener Granulomatosis	298
41.4	Crohn Disease	300
41.5	IgG4-Associated Multifocal Systemic Fibrosis	300
42	Pituitary Abscess	303
43	Empty Sella	307

44	Sheehan Syndrome	315
45	Pituitary Hyperplasia and Primary Hypothyroidism	319
46	Intracranial Hypotension Syndrome	323
47	Pituitary Hemochromatosis	327
48	Arachnoid Cyst	329
49	Epidermoid Cyst	333
50	Dermoid Cyst	337
51	Neurenteric Cyst	341
52	“Incidentalomas”. Posterior Pituitary Cyst	343
53	The Ectopic Posterior Lobe	347
54	Lipoma	355
55	Rare T1 Hyperintensities of the Anterior Pituitary Gland . . .	359
56	Craniopharyngeal Canal and Meningocele	363
57	Pituitary Gland Duplication and Triplication	367
58	The Sellar Spine	371
59	Vascular Variants of the Sellar Region	375
	59.1 Persistent Trigeminal Artery	375
	59.2 Intrasphenoidal Internal Carotid Artery	376
	59.3 Inferior Intercavernous Sinus.	376
	59.4 Intrasellar Internal Carotid Artery	377
60	Aneurysms	379
61	Trauma of the Pituitary Region	385
	Index	389

Abbreviations

3D TOF	3-dimensional time-of-flight
AC	arachnoid cyst
ACTH	adrenocorticotrophic hormone
ADC	apparent diffusion coefficient
ADH	antidiuretic hormone
AIP	aryl hydrocarbon receptor interacting protein
CE T1WI	contrast-enhanced T1-weighted image
CISS	constructive interference in steady state
CNS	central nervous system
CPC	craniopharyngeal canal
CSF	cerebrospinal fluid
CT	computed tomography
DWI	diffusion-weighted image
FLAIR	fluid-attenuated inversion recovery
FSH	follicle-stimulating hormone
GCT	granular cell tumor
GE	gradient echo
GH	growth hormone
LH	luteinizing hormone
MEN 1	multiple endocrine neoplasia type 1
MRA	magnetic resonance angiography
MRI	magnetic resonance imaging
PCNSL	primary central nervous system lymphoma
rCBV	relative cerebral blood volume
RCC	Rathke cleft cyst
ROI	region of interest
T1WI	T1-weighted image
T2WI	T2-weighted image
TSH	thyroid-stimulating hormone
WHO	World Health Organization

Collaborators

Michael Buchfelder, MD, PhD Professor of Neurosurgery, University of Erlangen-Nürnberg, Erlangen, Germany

Cyrine Drissi Faculty of Medicine, University of Tunis El Manar, Department of Neuroradiology, Institut National de Neurologie, Tunis, Tunisia

Julie Kreutz Department of Radiology, Centre Hospitalier Universitaire de Liège, Liège, Belgique

Maha Mahmoud Faculty of Medicine, University of Tunis El Manar, Department of Neuroradiology, Institut National de Neurologie, Tunis, Tunisia

Iulia Potorac Department of Endocrinology, Centre Hospitalier Universitaire de Liège, Liège, Belgique

Sven-Martin Schlaffer, MD Neurosurgeon, Department of Neurosurgery, University of Erlangen-Nürnberg, Erlangen, Germany

Françoise Cattin

1.1 Basic MRI Sequences

Three basic sequences are indicated in all clinical situations. These sequences are often adequate for the diagnosis, particularly in the search for microprolactinomas. Additional sequences may be obtained according to the clinical and biological status and after reading the basic sequences.

Sagittal T1W sequence focused on the pituitary region constitutes the first step of the MR examination: this sequence is rarely informative in the diagnosis of intrasellar lesions, but allows one to draw an anatomical plane, for example the sub-callosal plane, which will allow perfect reproducibility of the coronal cuts for serial MRI (Fig. 1.1). This sagittal T1W sequence is essential in the evaluation of lesions with suprasellar extension to analyze the anatomical surroundings. At 3.0 T, sagittal spin echo T1WI are obtained with the following parameters: TR/TE: 425/14, BW: 31,25 kHz, FOV/matrix: 23 cm/416×256, 3.0 mm thk/0.3sp, 3NEX, AT: 5:29. Standard protocol includes a coronal fast spin-echo T2W sequence (TR/TE: 3500/140, BW: 25 kHz, FOV/matrix: 20 cm/384×384, 2 mm thk/0.2sp, 4 NEX, AT: 5:15 and a coronal spin-echo T1W sequence (TR/TE: 700/14, BW: 31,25, FOV/matrix: 23 cm/416×256, 3 mm thk/0.2sp, 3 NEX, AT: 6:53) (Fig. 1.2).

When an intrasellar lesion is suspected on the sequences without contrast, the diagnosis can be confirmed by the realization of coronal T1WI after gadolinium injection (CE T1WI). A low

dose of contrast medium (0.05 mmol/k) is recommended to avoid a too intense enhancement, which may hide a small intraglandular lesion. Nevertheless, it is our own policy to spare gadolinium administration when the clinical situation is clear and confirmed by the noncontrast T1 and T2WI, for instance when searching for microprolactinomas. Delayed imaging 45 min after gadolinium injection can have some interest, mainly in Cushing disease, in revealing a very small microadenoma (“picoadenoma”) when T1, T2, and CE T1WI are not informative.

In the case of a lesion with suprasellar extension, coronal and sagittal T1W sequence after gadolinium injection and, if necessary, a 3D gradient echo T1W acquisition with gadolinium for neurosurgical planning are performed.

1.2 Additional Sequences

Axial TWI, preferentially with fat saturation is the best sequence to evaluate the storage of vasopressin and is thus highly recommended for the exploration of diabetes insipidus. This sequence will also be extremely useful to consolidate the diagnosis of intrasellar Rathke cleft cyst even when associated with pituitary microadenoma.

In the exploration of Cushing disease, if the standard sequences including the sequences after gadolinium injection are negative, a dynamic imaging is obtained (Fig. 1.3). A 3D T1W gradient-echo sequence with inframillimetric section

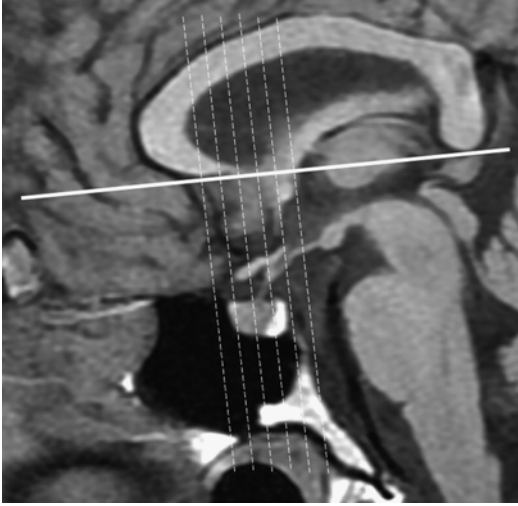


Fig. 1.1 Sagittal T1WI. The coronal cuts are obtained perpendicularly to the sub-callosal plane

thickness may demonstrate a tiny ACTH-secreting pituitary microadenoma.

3D TOF MRA is useful in the lesions affecting the cavernous sinus, particularly in the diagnosis of aneurysm of the intracavernous internal carotid artery, ectatic carotid siphons, and dural fistula, or to confirm anatomical variations such as persistent trigeminal artery.

1.3 Advanced MRI Techniques

Diffusion imaging, perfusion imaging, and proton MR spectroscopy (MRs) can be helpful in differentiating various types of lesions involving pituitary gland and hypothalamus. These techniques require the positioning of a region of interest (ROI) with a sufficient size, and thus may have a role only in the evaluation of large lesions.

Diffusion imaging can have an interest in early detection of pituitary infarction or pituitary apoplexy and in differentiation of abscess from hemorrhage, the ADC value being considerably decreased in pituitary ischemia and abscess. The relationship between diffusion imaging and apparent diffusion coefficient on one hand, and consistency of the pituitary adenoma on the other, is controversial. For some

authors, macroadenomas with hypersignal on diffusion imaging and a low ADC value present a soft consistency, while those with hyposignal and a high ADC value are firmer: these data may have been useful for the neurosurgeon but are not confirmed in recent studies. It is generally admitted today that there is no correlation between the ADC and both the consistency and secretory type of the pituitary adenoma.

MRs has a limited interest in the diagnosis of pituitary lesions. However, some MRs patterns can help to confirm a diagnosis evoked on standard sequences. Hypothalamic gliomas demonstrate increased choline peak and decreased N-acetylaspartate (NAA) peak. In craniopharyngiomas and germinomas, a high level of lipids is usually observed with only some traces of other metabolites. Hypothalamic hamartomas are characterized by decreased NAA and increased myoinositol. Pituitary adenomas can show only a choline peak; in the case of hemorrhagic complications, no metabolites are found.

1.4 Radiological Anatomy

1.4.1 The Anterior Lobe of the Pituitary Gland

In adults, the upper pole of the anterior lobe can be plane, concave, or convex. The signal of the normal anterior lobe is homogeneous, similar to that of the white matter of the temporal lobe on T1WI. A possible discrepancy between the size of the sella turcica and that of the pituitary gland can lead to mistakes. When the sella turcica is unusually small, the pituitary gland may appear bulky, overflowing frankly the theoretical plan of the sellar diaphragm in the manner of a brioche leaving its mold.

The size and morphology of the anterior lobe of the pituitary gland are variable according to age and sex (Fig. 1.4).

In the newborn and up to the end of the second month of life, the pituitary gland is rounder and larger than in the older child : 63 % of infants aged less than 1 month present a convex pituitary

gland against only 4 % of the children older than 2 months.

Before 2 months, the anterior lobe of the pituitary gland appears hyperintense on T1WI in 75 % of the cases if compared with the brainstem. This hypersignal is never observed beyond the second month. This hypersignal is

related to an increase of endoplasmic reticulum and intense activity of protein synthesis. The relatively large size of the pituitary gland at birth is correlated with hyperplasia of prolactin cells, an intense endocrinal activity and an important protein synthesis. Lack of high signal or discovery of a small pituitary gland in a

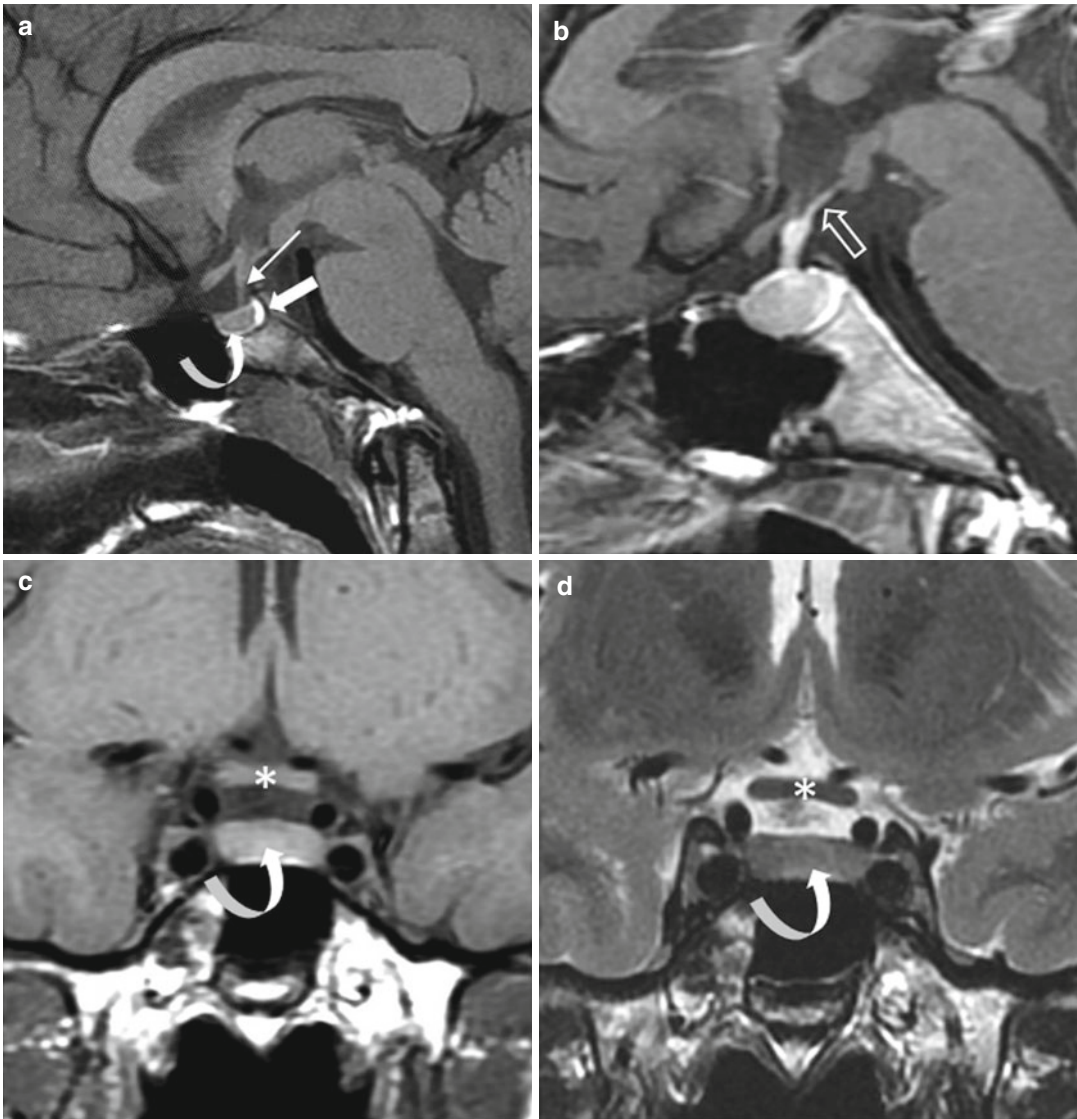


Fig. 1.2 Normal pituitary gland. (a, b) Sagittal T1 and CE T1WIs. (c, d) Coronal T1 and T2 WIs at the anterior part of the pituitary gland. (e, f) Coronal T1 and T2 WIs, 2 mm posterior to (c) and (d). Anterior lobe (*curved arrow*). Posterior lobe (*thick arrow*). Pituitary stalk (*thin*

arrow). On T2WI, a flow artifact in the suprasellar cistern blurs the pituitary stalk. Optic chiasm (*asterisk*). After gadolinium injection (b), enhancement of anterior lobe, pituitary stalk, and tuber cinereum (*open arrow*)

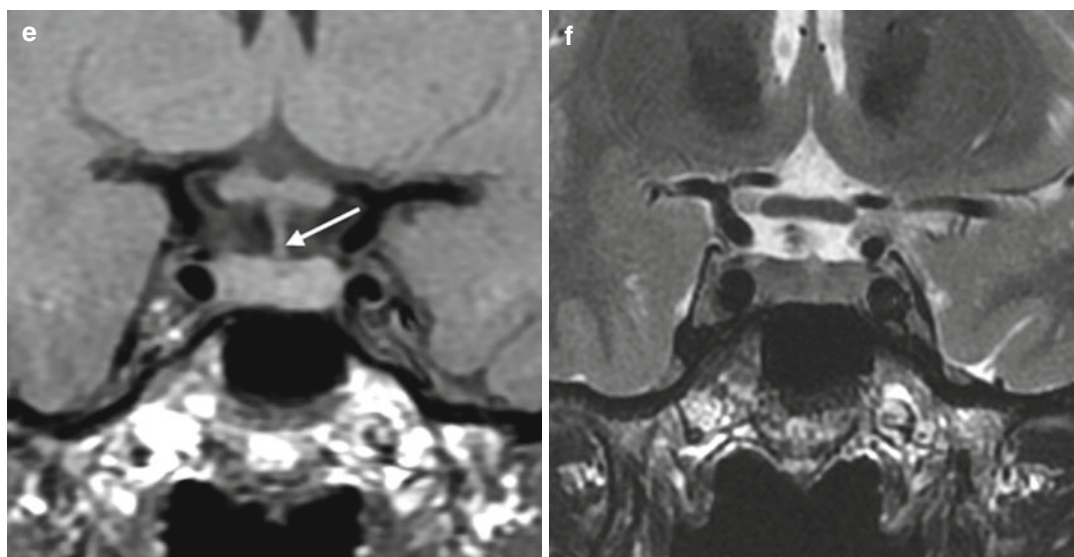


Fig. 1.2 (continued)

neonate should alert one to the possibility of pituitary malformation or dysfunction such as hypoglycemia. The usual hypersignal of the posterior lobe on T1WI is detectable from birth, so that the pituitary gland of the newborn appears entirely hyperintense.

Beyond 2 months of age, the pituitary gland tends to flatten and the signal of the anterior lobe becomes similar to that seen in the adult; the posterior lobe only remains hyperintense on T1WI. The height of the pituitary gland measured on the midsagittal plane is usually between 2 and 6 mm, and there is no difference between males and females.

At puberty, a physiological hypertrophy of the gland is visible in females and males, but is definitely more marked in females. Before 12 years, the pituitary gland does not measure more than 6 mm in height. At puberty, a pituitary gland height from 8 to 10 mm is not rare in females. In males, a height higher than 7 mm must be regarded as suspect. The upper pole of the pituitary gland is upwardly convex in 56 % of females at puberty versus 18 % in the other age groups. Thus, the increase in volume and T1 hypersignal of the pituitary gland occurs during the maximal hormonal secretion period.

In women less than 50 years old, the pituitary gland is larger than in men and is more often upwardly convex. The height of the pituitary gland is more than 7 mm in 1 out of 4 women; between 20 and 40 years, 58 % of women have a pituitary gland more than 7 mm in height. In men, the height of the pituitary gland decreases regularly between 20 and 65 years; only 10 % of men have a pituitary gland more than 6 mm in height, and only 3 % a pituitary height greater than 7 mm. In the elderly population, interstitial and perivascular fibrosis can lead to an empty sella, most of the time without major influence on pituitary function. Small deposits of amyloid and iron may be observed.

After gadolinium injection, the enhancement of the anterior lobe of the pituitary gland is usually intense and homogeneous. On dynamic imaging, the anterior lobe is opacified later than in the posterior lobe because of its predominantly portal blood supply. Temporal resolution of dynamic imaging of the pituitary gland is longer than that of a dynamic CT scan. The first image is obtained 20–30 s after the beginning of gadolinium injection, and shows opacification of the pituitary stalk and upper

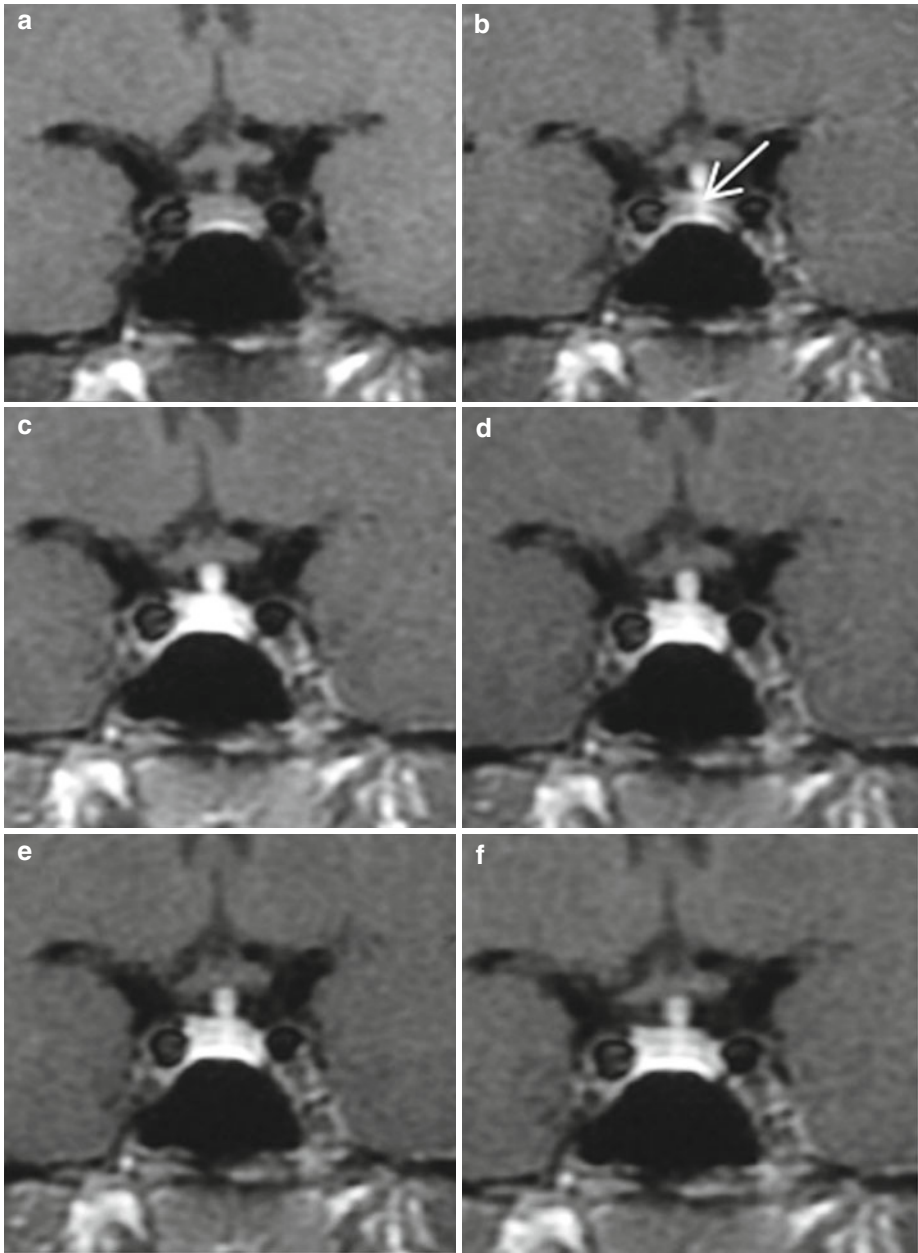


Fig. 1.3 Dynamic MRI of the normal pituitary gland. (a) Before contrast injection. (b) About 30 s later, opacification of the pituitary stalk and the secondary capillary bed (arrow). (c) At 60 s, the enhancement of the pituitary gland is intense and homogeneous. (d–f) Slow decrease of enhancement intensity

part of the pituitary gland corresponding to the secondary pituitary capillary bed (“tuft”) and the adjacent glandular parenchyma already contaminated by gadolinium. On the second

image at 40–60 s after gadolinium, the pituitary gland is intensely and homogeneously opacified, after which a slow decrease of intensity is observed.

1.4.2 The Pituitary Stalk

Under normal conditions, the diameter of the upper part of the pituitary stalk is thicker than the lower part. Thus, a tube-like pituitary stalk may be an indicator of an abnormal pituitary stalk. A physiological elongation of the infundibular recess of the third ventricle can simulate an enlarged stalk. The maximal diameter of the pituitary stalk measured on the axial plane is about 3 mm. The pituitary stalk is not always vertical: a

more or less marked tilting is not infrequent. This anatomical variation confirms that the displacement of the pituitary stalk is not a highly reliable sign for the diagnosis of pituitary microadenoma.

1.4.3 The Posterior Lobe of the Pituitary Gland

It is currently well established that the hyper-signal visible on T1WI and located at the poste-

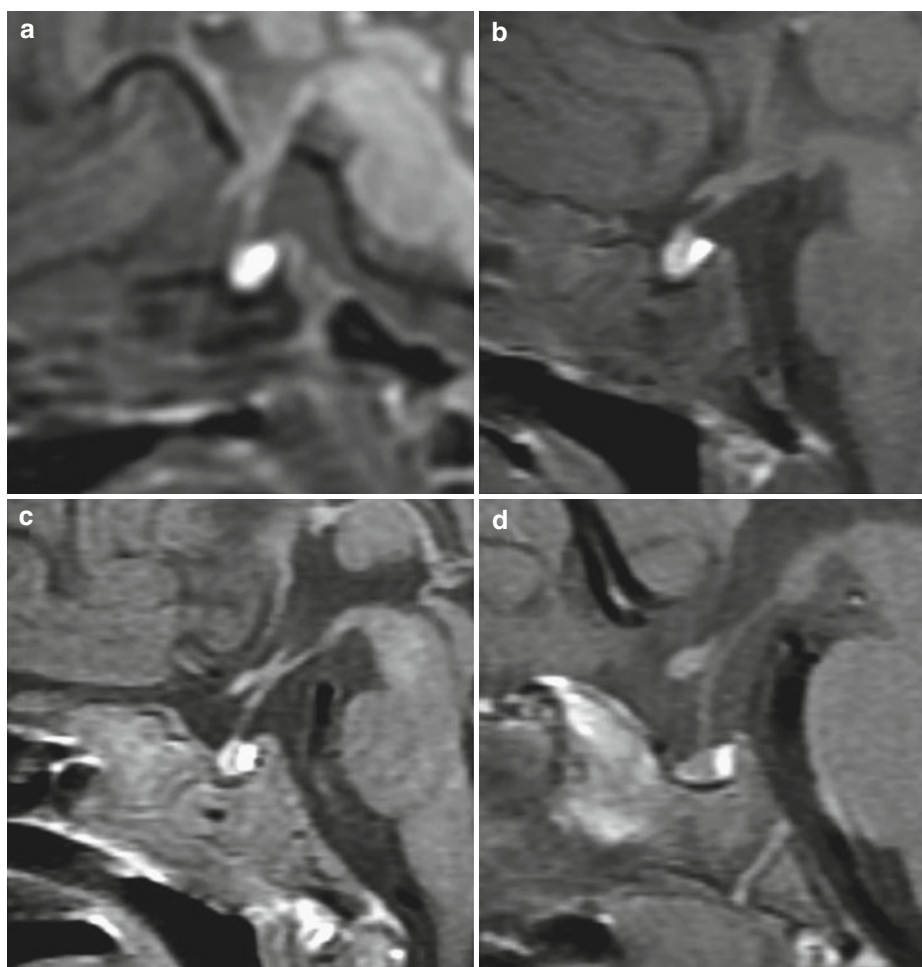


Fig. 1.4 Pituitary gland in children, sagittal T1WIs. (a) 5-day-old newborn. Round and globulous pituitary gland. Anterior pituitary is markedly hyperintense and indistinguishable from the posterior lobe. (b) 12-day-old newborn. The convex anterior pituitary is hyperintense but slightly less so than the posterior pituitary. (c) 7-week-old infant. Convex upper pole of the pituitary gland.

Hyperintensity of the anterior pituitary is less marked than that of the posterior pituitary. (d) 21-month-old child. The anterior pituitary gland is no more hyperintense. The posterior lobe is proportionally larger than in adult. (e) 7-year-old boy. No change when compared with (d). (f) 15-year-old girl. Normal convex pituitary gland of the adolescent

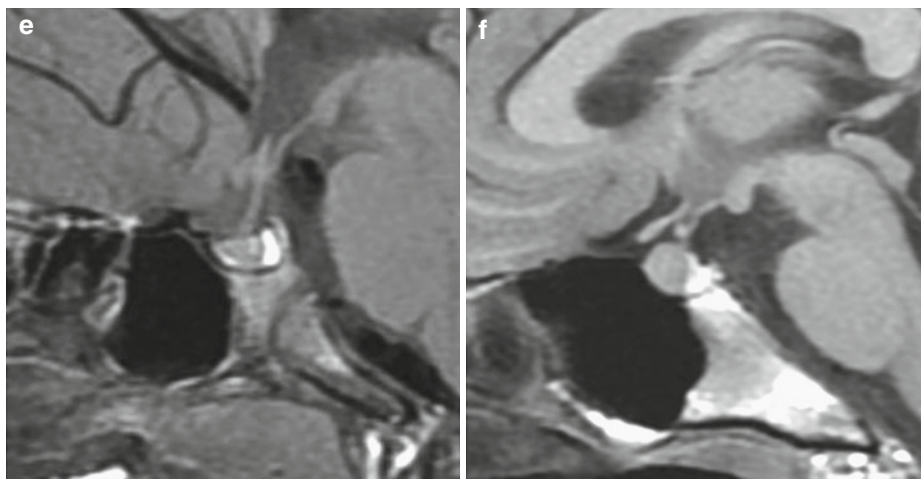


Fig. 1.4 (continued)

rior part of the sella turcica corresponds to the storage of vasopressin in the posterior lobe. This T1 hypersignal indicates a normal functional state of the posterior lobe. The T1 hypersignal disappears in patients with central diabetes insipidus. An exact explanation of this T1 hypersignal is as yet not available. For some authors, the hypersignal is in relation with lipidic droplets present in the pituicytes. For others, the hypersignal corresponds to the antidiuretic hormone (ADH) granules or to a complex of ADH and neurophysin. A third theory states that the hypersignal is related to the presence of phospholipids in the posterior lobe of the pituitary gland.

Lack of visualization of the posterior lobe on the sagittal plane in normal subjects is generally due to an inappropriate technique, or to anatomical reasons such as a fatty or thick dorsum sellae. Realization of axial cuts allows one to reach a rate of detection of the posterior lobe close to 100 %. Classically, the posterior lobe is described on sagittal images as a hyperintense and homogeneous structure with regular anterior convexity, in contact with the dorsum sellae (Fig. 1.5). In fact, this pattern is not always seen: heterogeneous signal and irregularities of the anterior aspect of the posterior lobe, which could suggest an irregular distribution of the

neurosecretory granules, are frequently observed. In the elderly, the signal of the posterior lobe is less intense and often heterogeneous, as a result of the persistently raised plasmatic osmolality (Fig. 1.6). For the same reason, lesser T1 hyperintensity can be observed during pregnancy, in patients undergoing hemodialysis or with uncontrolled diabetes mellitus, severe anorexia nervosa, and in a stressed condition.

Cysts are rarely encountered in the posterior lobe. They appear on axial T1WI without contrast as T1-hypointense clefts surrounded by a T1-hyperintense rim corresponding to normal vasopressin storage (Fig. 52.4).

1.4.4 The Cavernous Sinus

Before gadolinium injection, the internal carotid arteries present a hyposignal in T1 and T2 related to fast flow; this lack of signal is known as “flow void.”

Most venous elements of the cavernous sinus are located below and laterally to the internal carotid artery. When the internal carotid artery is remote to the wall of the sphenoid sinus, the vacant space is always filled by a vein, the vein of the carotid sulcus, or by several small veins.

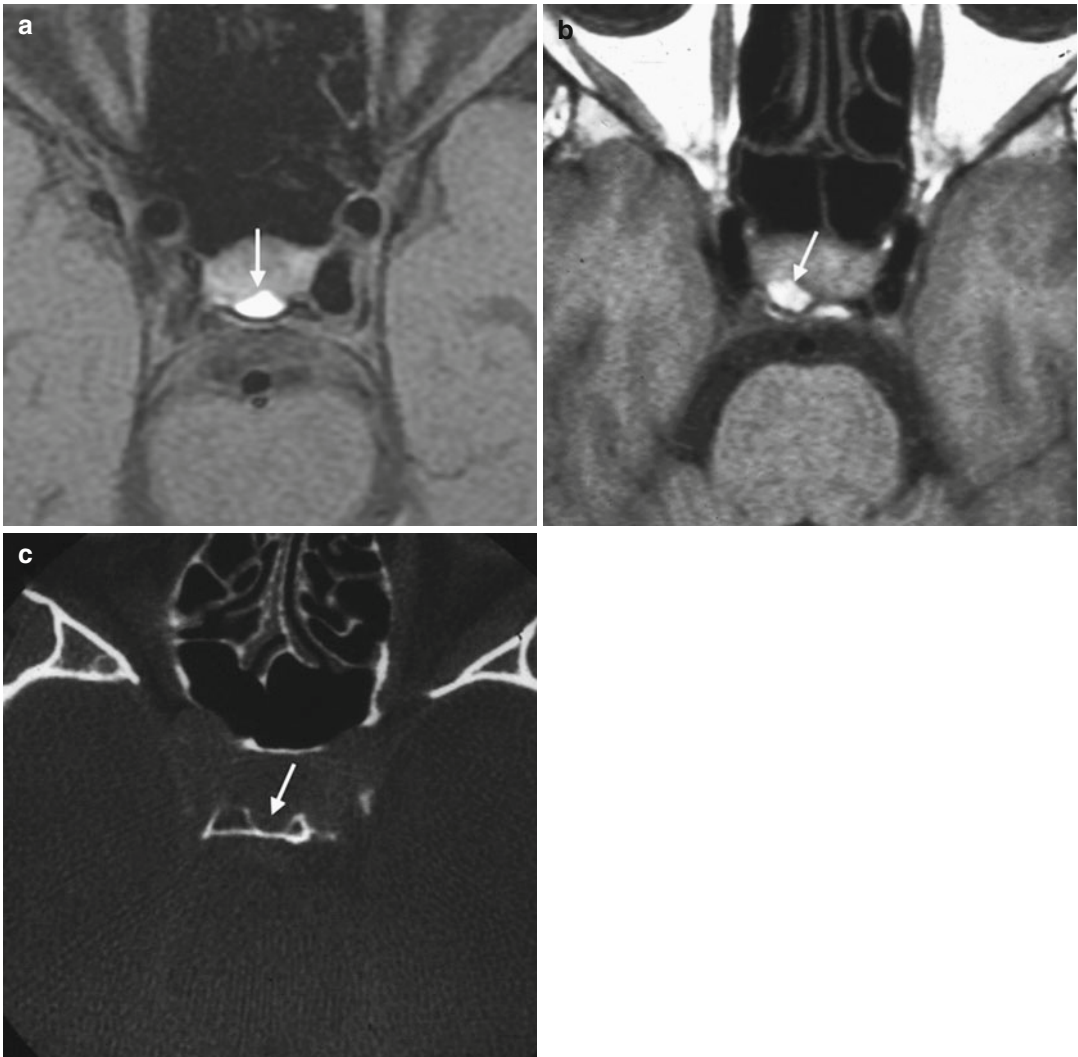


Fig. 1.5 Normal posterior lobe of the pituitary gland. (a) Axial Fat-Sat T1WI at 3.0 T. Suppression of the fat signal of the dorsum sellae allows good delineation of the hyperintense posterior lobe (*arrow*). (b) Axial T1WI at

1.5 T. Lateralized posterior lobe. (c) Axial CT scan, bone window demonstrating the imprint of the posterior lobe in the dorsum sellae (fossula hypophyseos) (*arrow*)

Lack of visualization of the vein of the carotid sulcus can be considered a reliable sign of invasion of the cavernous sinus by a pituitary adenoma.

The large veins with fast flow are hypointense on T1WI while the smaller veins with slow flow are hyperintense. Often one or more venous structures are visualized between the intracav-

ernous internal carotid artery and the pituitary gland, indicating the medial limit of the cavernous sinus. The inferior intercavernous sinus is frequently demonstrated in normal children. In adults, a prominent inferior intercavernous sinus leads to a search for an intracranial hypotension syndrome or a vascular malformation of the sellar region.

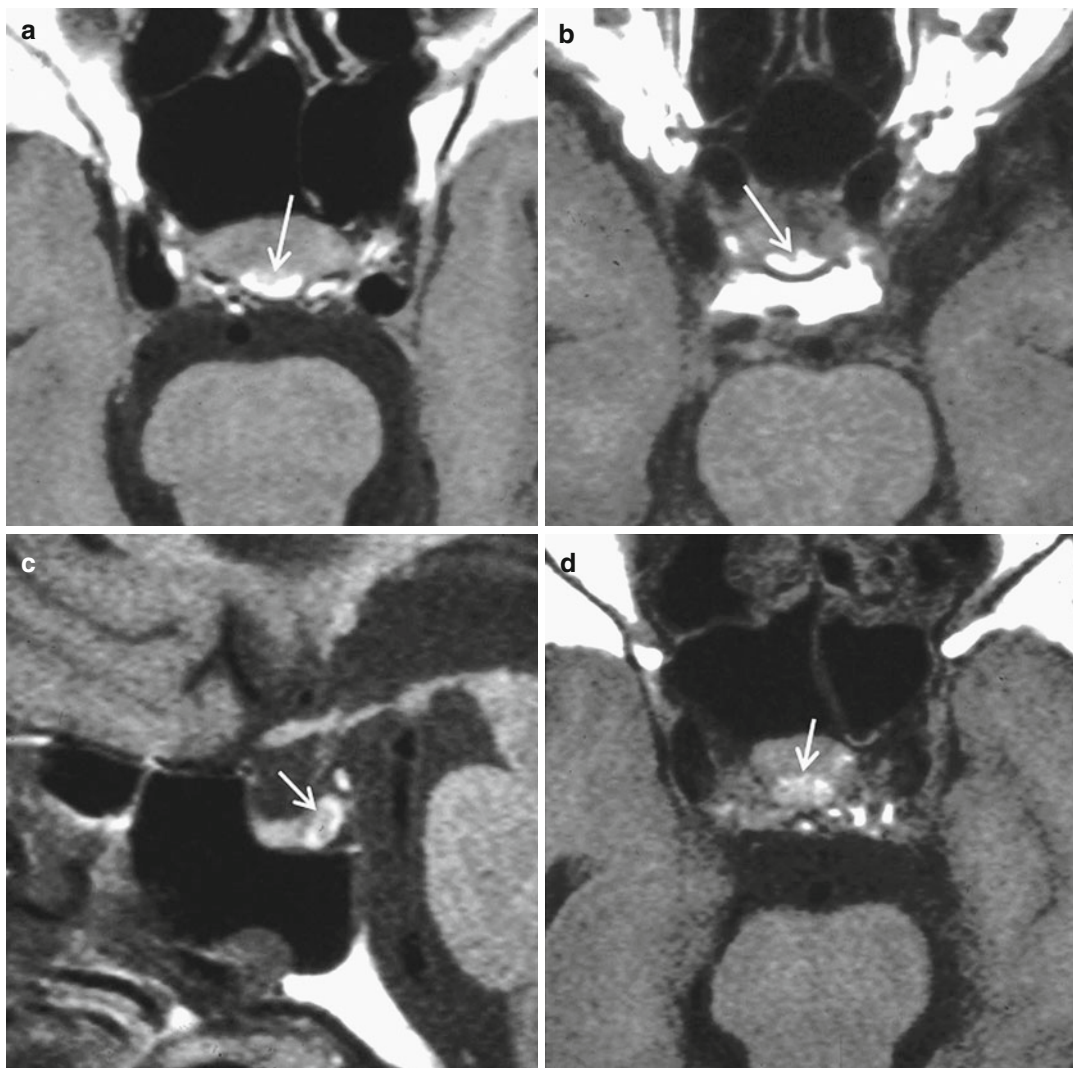


Fig. 1.6 Variants of posterior lobe. (a, b) Axial T1WIs in two elderly subjects. Heterogeneous appearance and irregularities of the anterior aspect of the posterior lobe

(arrow). (c, d) Axial T1WIs in a 78-year-old woman. The posterior lobe is faintly hyperintense (short arrow)

The intracavernous cranial nerves appear hypointense on T1WI relative to the other elements of the cavernous sinus, and are thus better visible when underlined by hyperintense veins. The oculomotor nerve is always identified in the upper compartment of the cavernous sinus. On T2WI, a hyperintense thin layer of CSF is often observed around the cranial nerves, in particular the oculomotor nerve. The dural layer separating

the pituitary gland from the cavernous sinus is extremely thin, particularly in the posterior part of the sella turcica. This layer is frequently visible on the coronal and, sometimes, axial T2WI at 3.0 T. The rupture of this membrane constitutes a direct sign of invasion of the cavernous sinus by a pituitary adenoma. The thicker lateral dural wall of the cavernous sinus is always identified, and markedly hypointense on T1WI and T2WI.

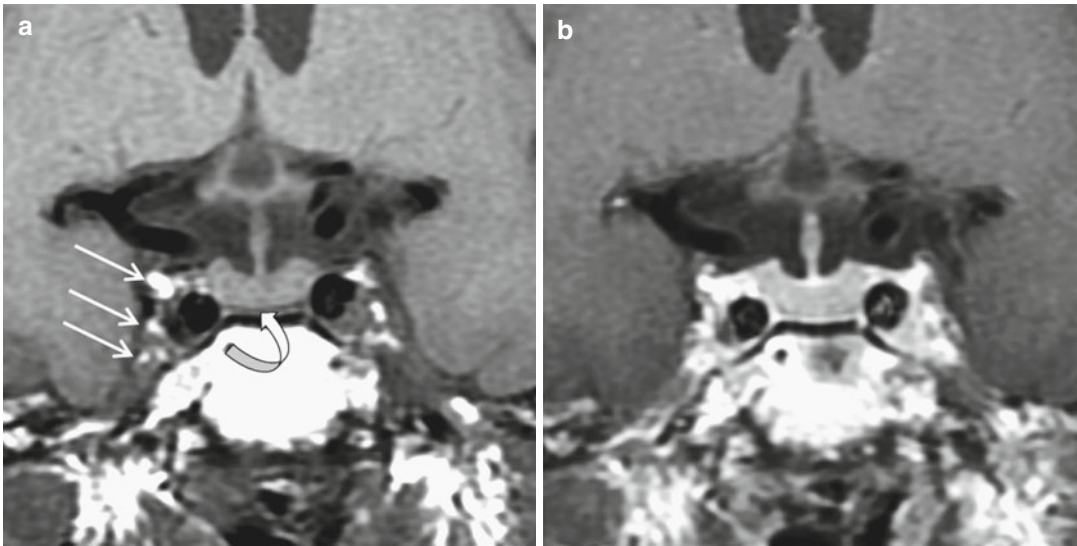


Fig. 1.7 Normal cavernous sinus. (a) Coronal T1WI and (b) CE T1WI. The low-flow veins appear hyperintense on T1WI and CE T1WI (*arrows*). A thin inferior intercavernous

sinus is demonstrated in contact with the sellar floor (*curved arrow*)

After gadolinium injection, the lumen of the intracavernous internal carotid arteries does not enhance on spin-echo T1WI. The T1-hypointense large veins usually enhance while there is no change of the spontaneously T1-hyperintense veins (Fig. 1.7). The dural lateral wall of the cavernous sinus intensely enhances. Later after gadolinium injection, the intracavernous internal carotid artery and the cranial nerves appear as hypointense structures within the quite homogeneous hyperintense cavernous sinus.

High-resolution spin-echo T1WI and fast spin-echo T2WI allow the visualization of the internal architecture of the Meckel cave. The tracts of nervous fibers that constitute the trigeminal nerve in the Meckel cave can be identified within the CSF, especially on T2WI (Fig. 1.8). In general, the trigeminal ganglion is visible laterally in the anterior part of the Meckel cave, as a semilunar or nodular structure taking up contrast. In the other cases, the trigeminal ganglion is incorporated with the lateral dural wall of the Meckel cave.

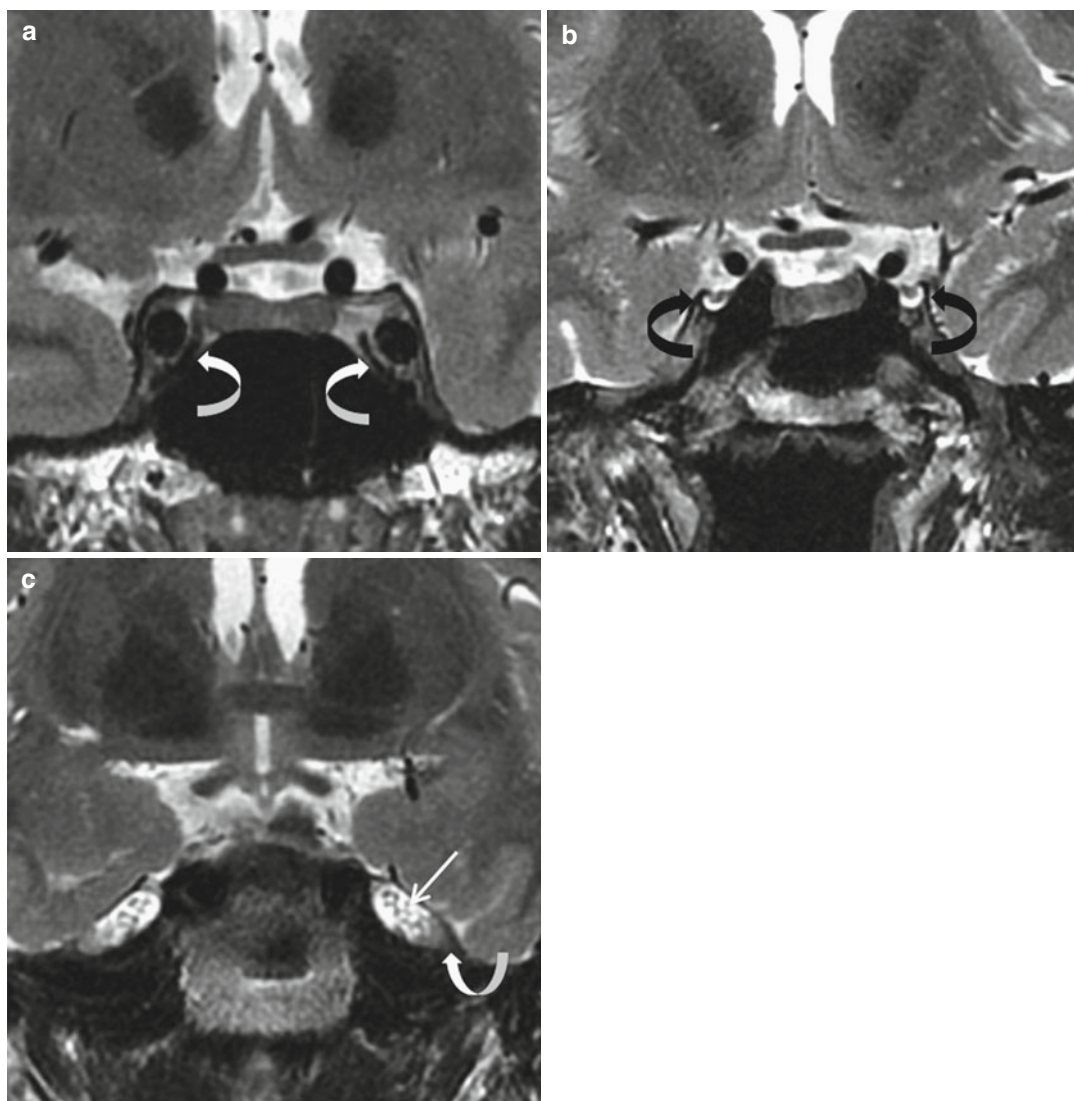


Fig. 1.8 Normal cavernous sinus. Coronal T2WIs. (a) Bilateral veins of the carotid sulcus located between the sphenoid sinus lateral wall and the intracavernous internal carotid artery (*curved arrows*). (b) The oculomotor nerves, well delineated by their CSF-filled sheaths, are

identified at the upper compartment of the cavernous sinus (*black curved arrows*). (c) Posterior cut through the Meckel cave. The tracts of nervous fibers constituting the trigeminal nerve (*arrow*) are seen in the CSF of both the Meckel cave and the trigeminal ganglia (*curved arrow*)

Further Reading

- Doraiswamy PM, Potts JM, Axelson DA et al (1992) MR assessment of pituitary gland morphology in healthy volunteers: age- and gender-related differences. *AJNR Am J Neuroradiol* 13:1295–1299
- Kucharczyk W, Lenkinski RE, Kucharczyk J, Henkelman RM (1990) The effect of phospholipid vesicles on the

NMR relaxation of water: an explanation for the MR appearance of the neurohypophysis? *AJNR Am J Neuroradiol* 11:693–700

- Tien RD, Kucharczyk J, Bessette J, Middleton M (1992) MR imaging of the pituitary gland in infants and children: changes in size, shape and MR signal with growth and development. *AJR Am J Roentgenol* 158:1151–1154

Jean-François Bonneville

Artifacts and traps constitute a daily source of difficulties and mistakes when reading MR images of the sellar region. If not recognized they can mimic intrasellar lesions, in particular pituitary microadenomas.

Partial volume artifacts occur when a 3-mm-thick section, for instance, includes different anatomical structures such as the anterior pituitary gland and the sphenoid sinus anteriorly, the dorsum sellae posteriorly, or the intracavernous internal carotid arteries laterally. The computer calculates the intensity average of the different components of the section and makes an image that can simulate an intrasellar tumor (Fig. 2.1). Partial volume effects can be eliminated by coupling orthogonal projections or by using 1 mm-thick cuts, for instance with a gradient-echo 3D technique. *Magnetic susceptibility artifacts* are responsible for geometrical distortion and localized signal intensity changes at the interface of anatomical structures of different signal intensities, mainly in the case of a curved interface. Magnetic susceptibility artifacts are often present at the planum sphenoidale or at the

sellar floor level; they are more pronounced at 3.0 T (Fig. 2.2) but can be cleared up with technical ploys. *Chemical shift artifacts* and ghosting are related to the high signal of fat; they can compromise the visualization of vasopressin storage in the posterior lobe on axial T1W sections when the dorsum sellae is fatty, particularly at 3.0 T. In this case fat saturation is very useful (Fig. 2.3).

Flow artifacts arise mainly out of pulsating internal carotid arteries and CSF. They are more marked at 3.0 T and can blur or pollute images of the pituitary fossa or subarachnoid space (Fig. 2.4). *The posterior lobe and a deep fossula hypophyseos* are frequently mistaken for a posteriorly located pituitary adenoma on coronal T2WIs (Fig. 2.5); topography of the posterior lobe, which is half of the time off-midline, is ideally demonstrated on axial T1W fat-saturated imaging. *Dynamic imaging* should not be performed routinely but only in specific cases. Its interpretation must be rigorous or it can lead to false-positive diagnoses (Fig. 15.5).

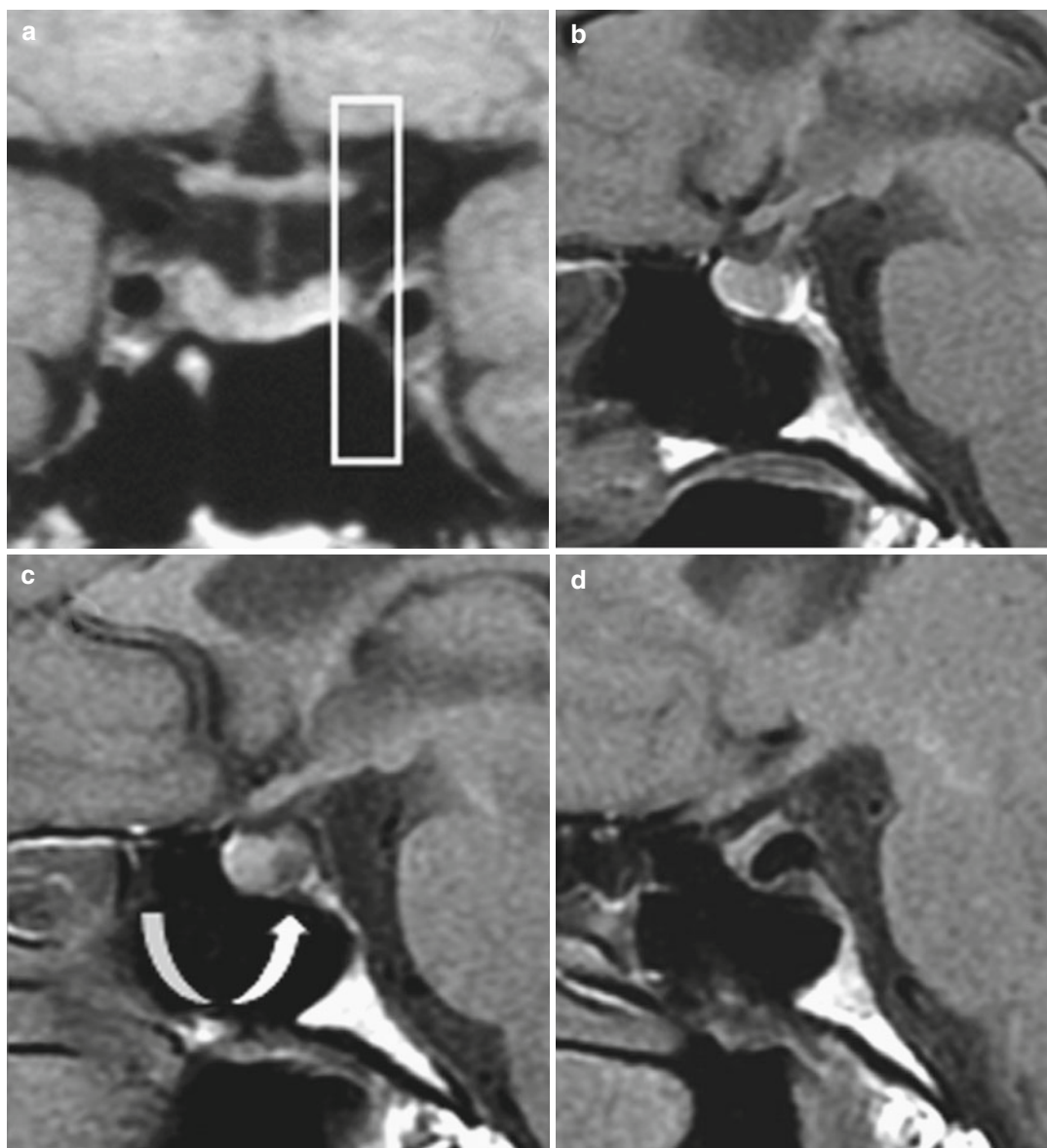


Fig. 2.1 Partial volume effect artifact. (a) Coronal T1WI. (b–d) Sagittal T1WIs. A thick section includes pituitary tissue and part of the intracavernous internal carotid

artery, with a resulting image simulating a pituitary adenoma (*arrow*)

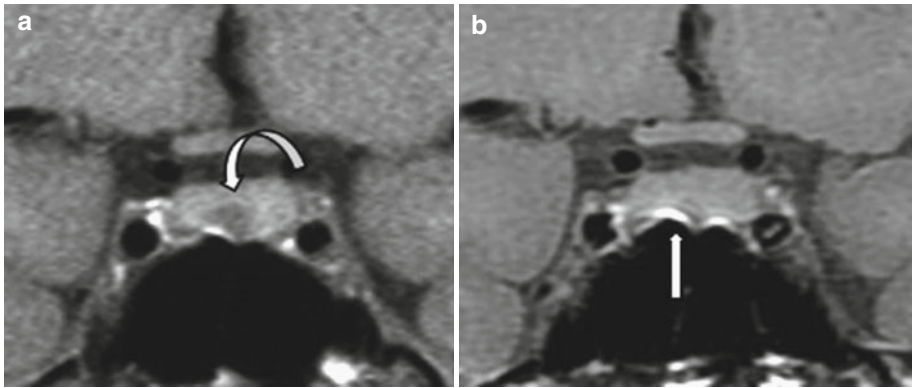


Fig. 2.2 Magnetic susceptibility artifact. (a) Coronal T1WI at 1.5 T demonstrates a 5-mm hypointense microadenoma (*curved arrow*). (b) T1WI at 3.0 T: the distortion of the sellar floor (*straight arrow*) masks the pituitary adenoma

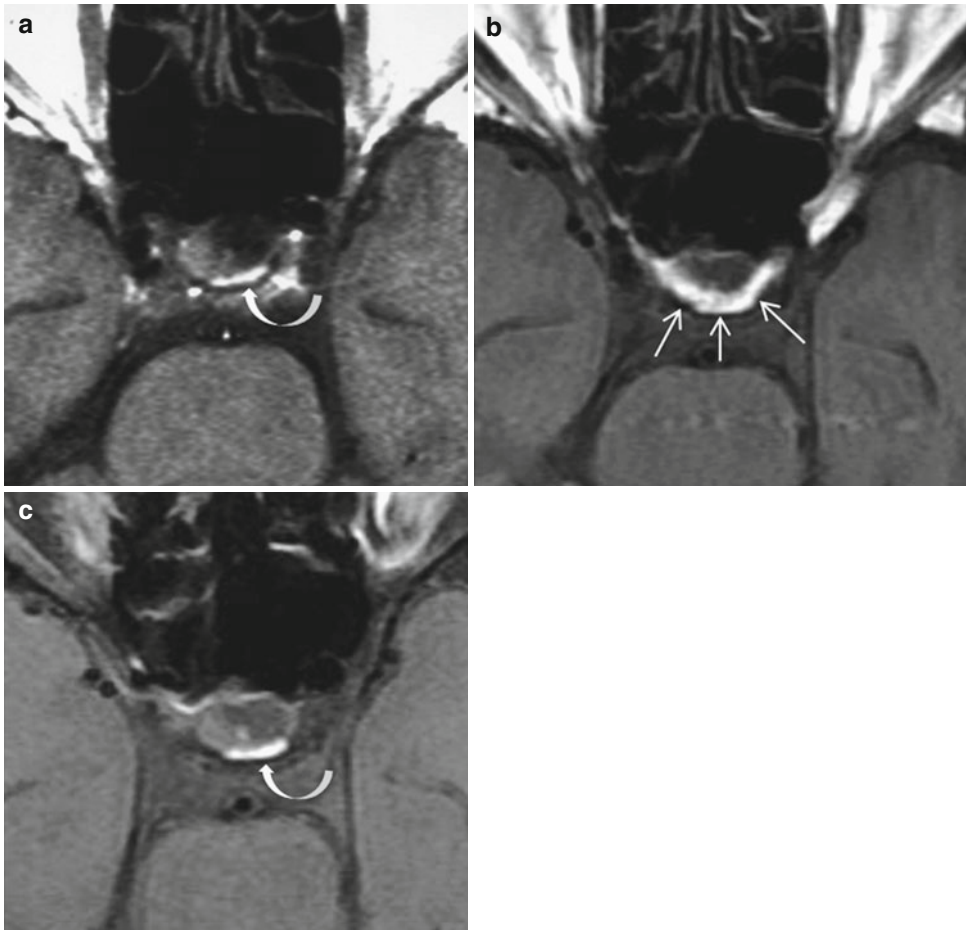


Fig. 2.3 Chemical shift artifact. (a) Axial T1WI at 1.5 T shows a normal T1-hyperintense posterior lobe (*curved arrow*). (b) Axial T1WI at 3.0 T fails to demonstrate the posterior lobe: the image of the fatty dorsum sellae is displaced forward and is superimposed on the posterior

lobe: chemical shift artifact (*straight arrows*). (c) Axial T1W fat-saturated image at 3.0 T: this sequence eliminates fat and permits localization of the antidiuretic hormone storage in the posterior lobe

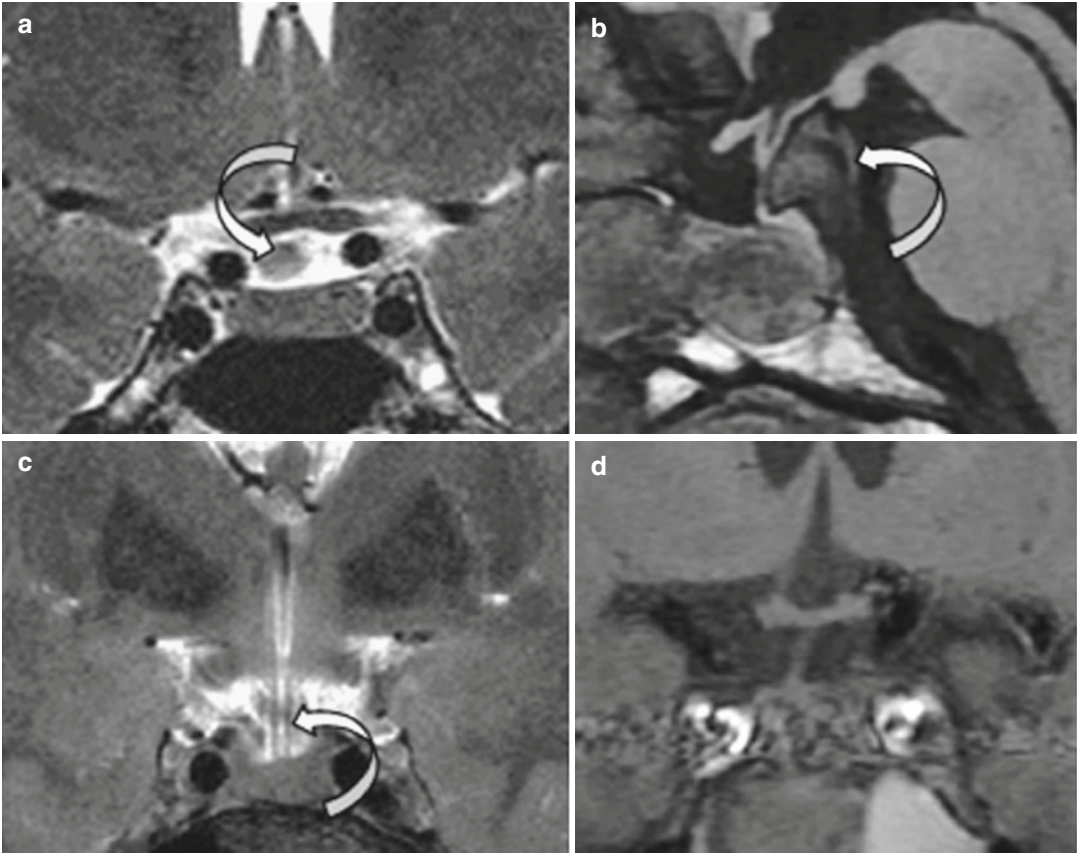


Fig. 2.4 Flow artifacts. (a) Coronal T2WI. (b) Sagittal T1WI. (c) Coronal T2WI. (d) Coronal T1WI. Flow artifacts from CSF (a–c) can be misleading, particularly in

the optochiasmatic cistern (*arrows*). Flow artifacts from the internal carotid arteries (d) can hinder visualization of the pituitary gland

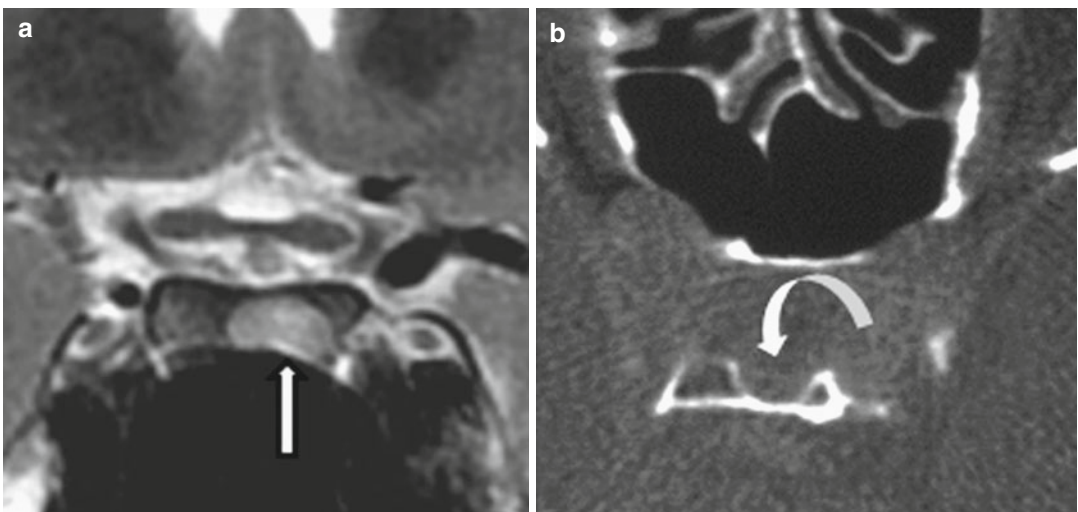


Fig. 2.5 Fossula hypophyseos and posterior lobe. (a) Coronal T2WI through the dorsum sellae. A rounded T2-hyperintense image (*arrow*) could mimic a pituitary

adenoma. (b) axial CT, bone window. This image is the result of a deep imprint of the dorsum sellae serving as a bed for the posterior pituitary (*curved arrow*)

Further Reading

- Bonneville JF, Bonneville F, Cattin F (2005) Magnetic resonance imaging of pituitary adenomas. *Eur Radiol* 15(3):543–548
- Elster AD (1993) Sellar susceptibility artifacts: theory and implications. *AJNR Am J Neuroradiol* 14(1):129–136
- Sakurai K, Fujita N, Harada K et al (1992) Magnetic susceptibility artifact in spin-echo MR imaging of the pituitary gland. *AJNR Am J Neuroradiol* 13(5):1301–1308

Jean-François Bonneville and Françoise Cattin

A small sella turcica is a normal anatomical variant responsible for an inadequacy between the sellar volume and its content, with a resultant bulging of the pituitary gland. It can mimic a pathological enlargement of the pituitary gland and, if not recognized, can lead to a false diagnosis of “pituitary hyperplasia” or even pituitary tumor. This is particularly true in teenage females with physiological enlargement of the pituitary gland.

In adults, a small sella turcica is frequently related to a hyperpneumatization of the sphenoid sinus. It feels like excessive pneumatization of the sphenoid sinus inhibits the complete development of the pituitary fossa. Hyperpneumatization of the sphenoid sinus may be associated with a flat or narrow sella and a resultant bulging of the pituitary gland.

A thick dorsum sellae, either pneumatized or fatty, can restrict the anteroposterior diameter of the pituitary fossa. The sella turcica can also be short transversally. This condition is difficult to apprehend: we must bear in mind that only 2 out of 100 adults have a sellar floor width of less than 10 mm. Therefore, an upward convex pituitary gland above a sella floor less than 10 mm wide is very likely to be an anatomical variant (Fig. 3.1).

In summary, in front of what looks like an enlarged pituitary gland with normal T1 and T2 signals and normal enhancement after gadolinium injection, a small sella has to be evoked: for

instance, in the case of unusual hyperpneumatization of the sphenoid sinus, such as pneumatization extending beyond the spheno-occipital synchondrosis or deep in the pterygoid processes. Asymmetrical hyperpneumatization may be particularly misleading (Fig. 3.2). Blistering of the planum sphenoidale also accompanies sphenoid sinus hyperpneumatization (Fig. 3.3). The shape of the dorsum sellae and the sellar width must also be carefully scrutinized.

Differential diagnosis of an upward bulging of the pituitary gland includes mainly the holosellar pituitary adenoma. In the latter, the posterior lobe appears compressed on axial T1WI, but not in the case of a bulging normal pituitary gland above a small sella turcica. An ignored or masked pregnancy in women of child-bearing age must also be kept in mind: T1 hyperintensity of the pituitary gland, if compared with the pons on sagittal T1WI, will make the diagnosis beyond the second trimester of the pregnancy. The useful volume of a normal-sized sella can also rarely be reduced by an unusually large inferior coronary sinus, for instance, “kissing” internal carotid arteries (Fig. 56.5) or a sellar spine (Fig. 3.4). Finally, several factors can be associated with reduction in sellar volume (Fig. 3.5). Conversely, a small sella or a narrowed sellar volume are not necessarily associated with an upward bulging of the pituitary gland.

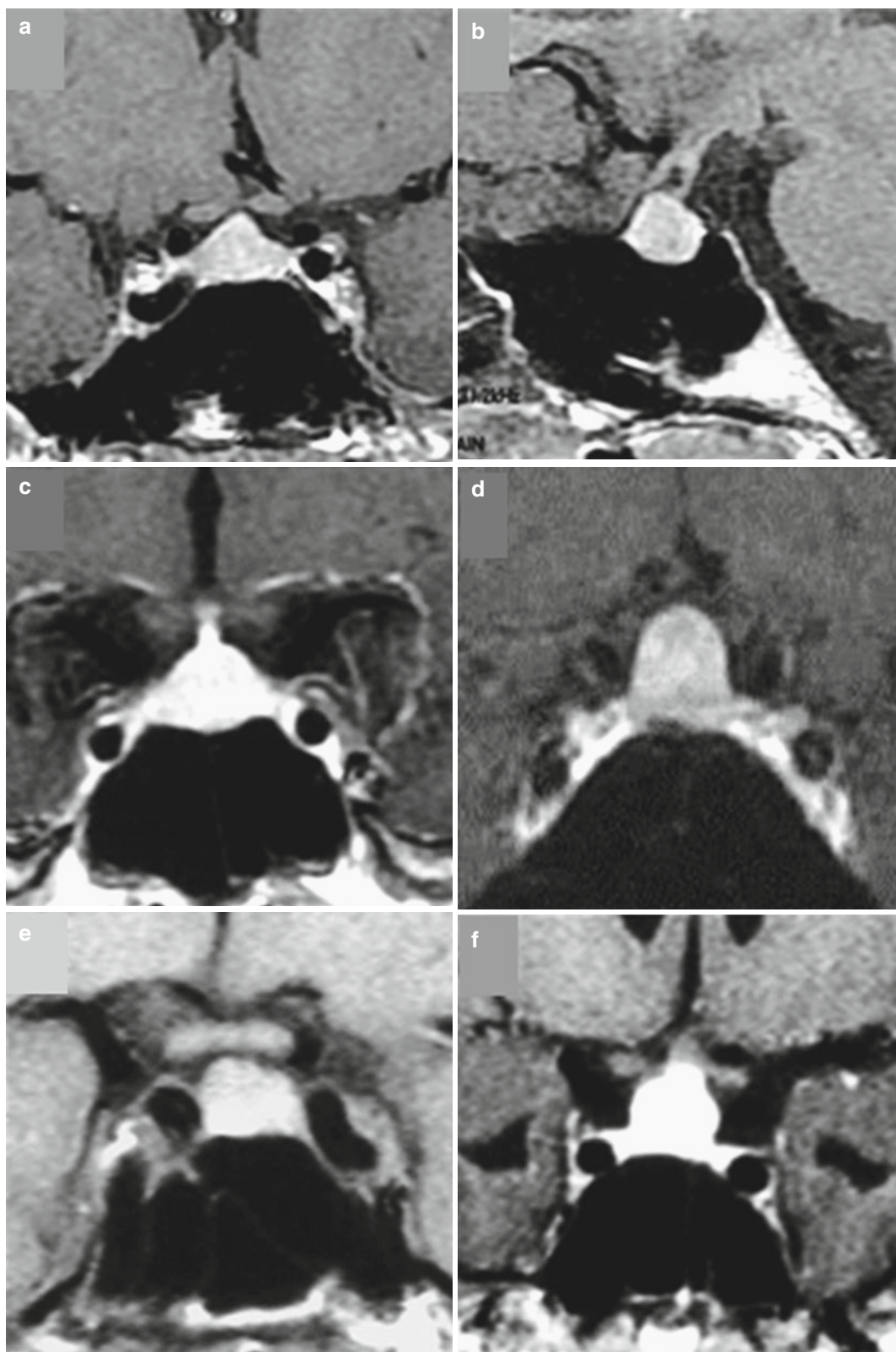


Fig. 3.1 (a, b) Physiological bulging of the pituitary gland on coronal and sagittal CE T1WI. (c–f) Coronal CE T1WI. Small sella, hyperpneumatization of the sphenoid sinus, and/or narrow sellar floor

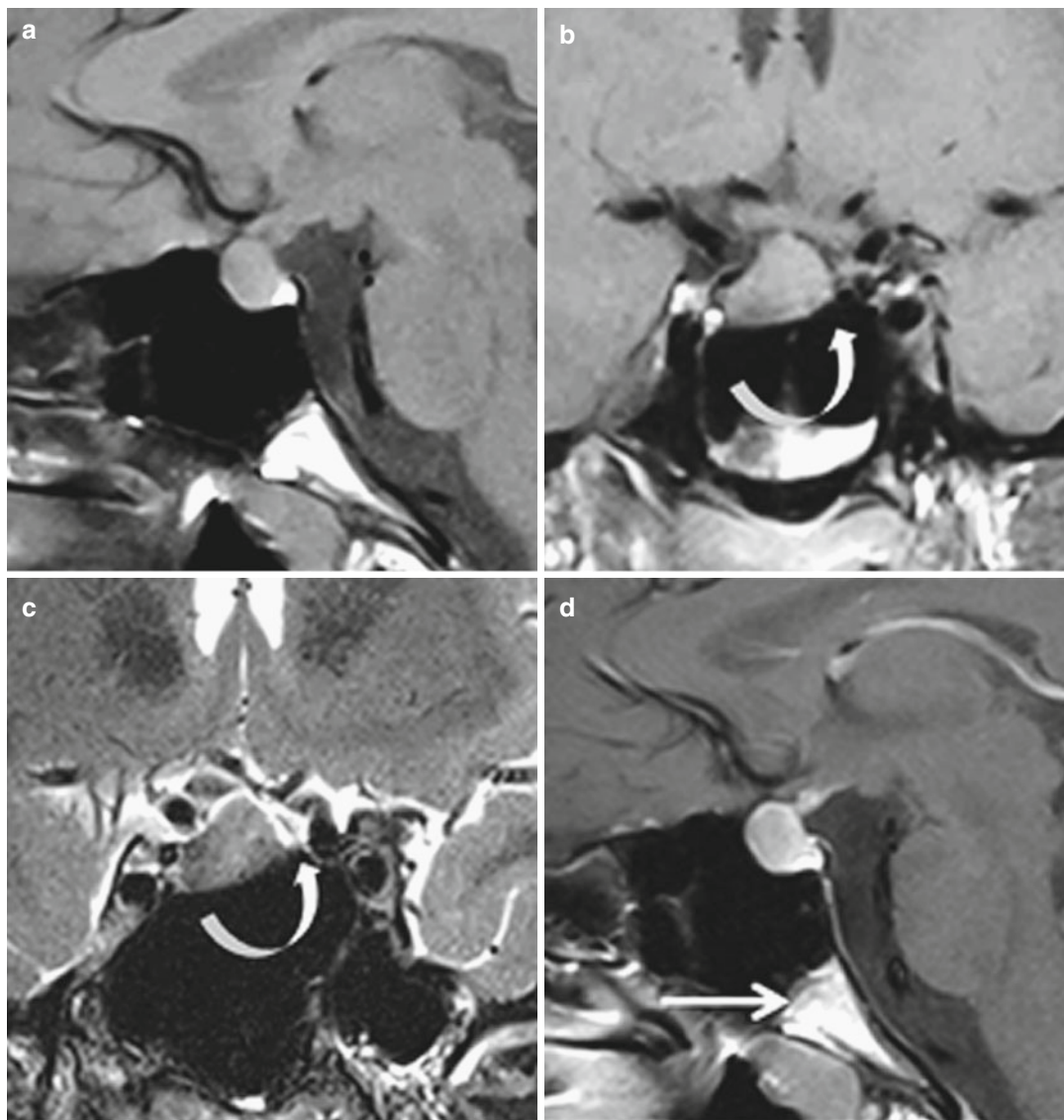


Fig. 3.2 Physiological bulging of the pituitary gland in a 16-year-old girl. Asymmetrical hyperpneumatization. (a, d) Sagittal T1 and CE TIWIs. (b, e) Coronal T1 and CET1WIs. (c) coronal T2WI. (f) Axial CE TIWI. Sphenoid

sinus pneumatization reaches the spheno-occipital synchondrosis (*arrow*). Excessive pneumatization on the left side (*curved arrows*) pushes the pituitary gland upward and to the right

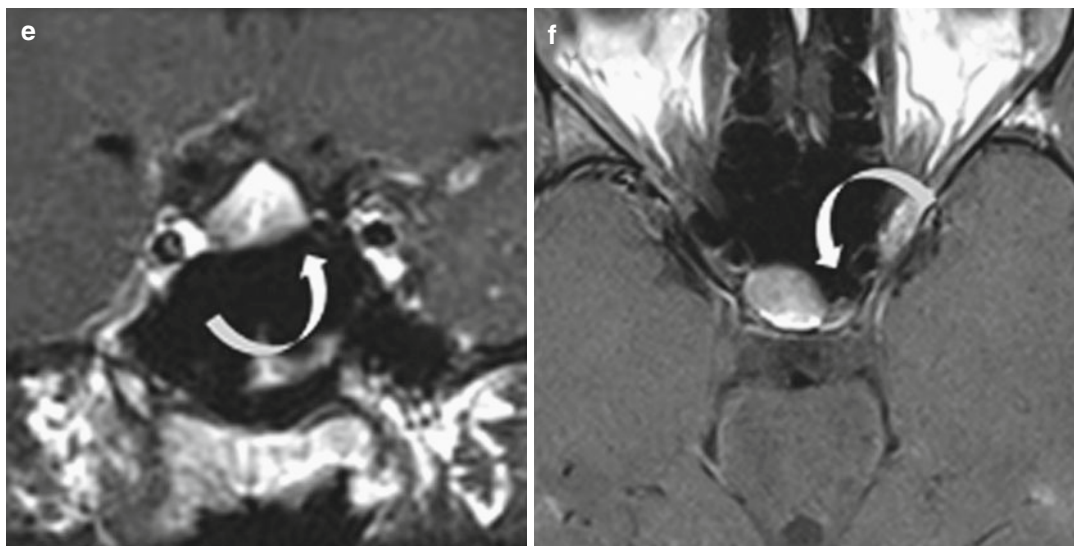


Fig. 3.2 (continued)

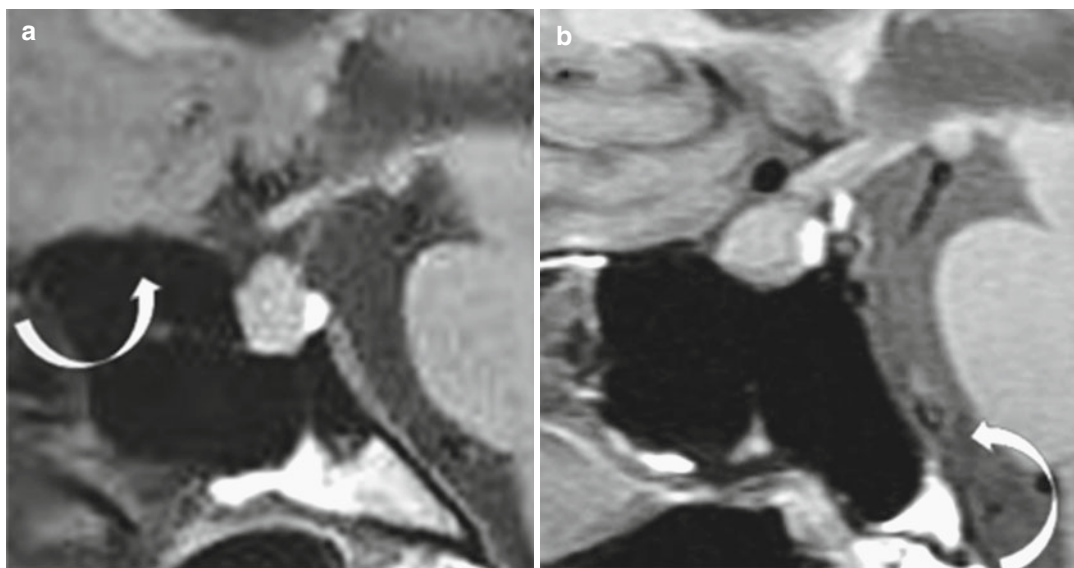


Fig. 3.3 Physiological bulging of the pituitary gland; small sella and hyperpneumatization of the sphenoid sinus. (a, b) Sagittal T1WI. (a) Blistering of the planum

sphenoidale (*arrow*). (b) extension of the pneumatization beyond the sphenoidale (*arrow*)

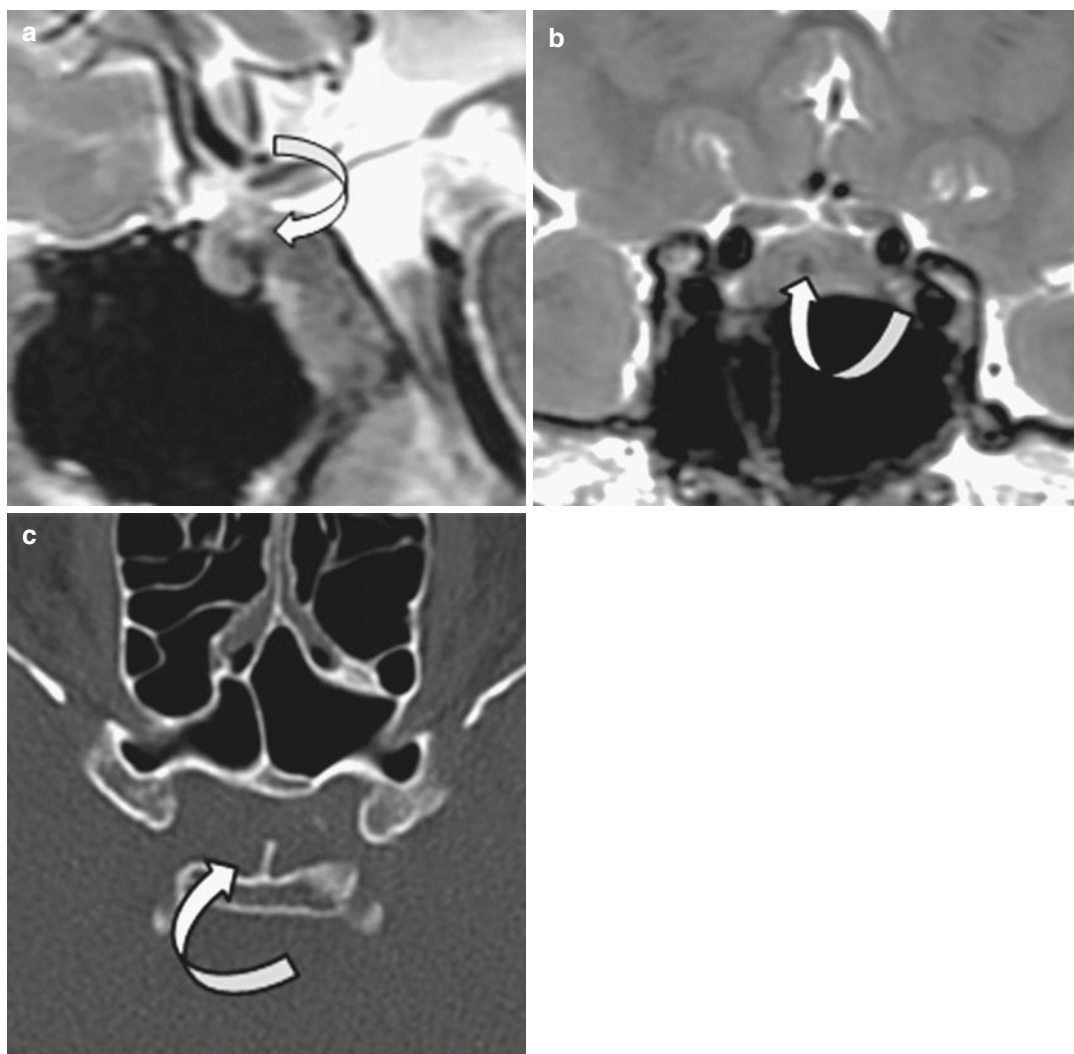


Fig. 3.4 Sellar spine (*arrow*) arising from the dorsum sellae and pushing the pituitary gland upward. (**a, b**) Sagittal and coronal T2WIs. (**c**) Axial CT

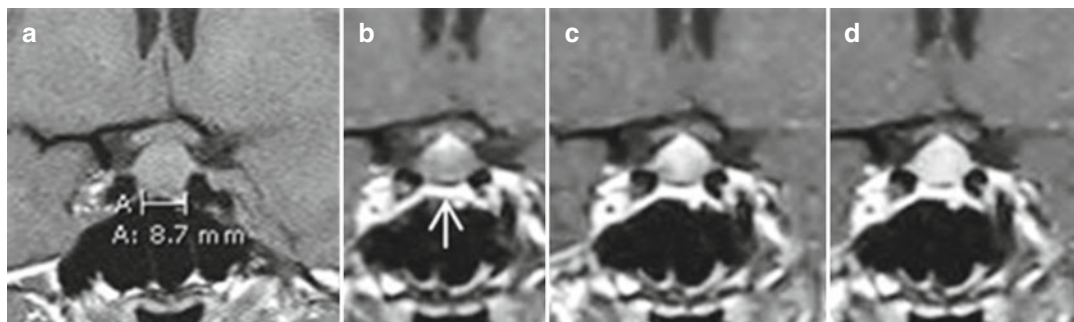


Fig. 3.5 Upward bulging of the upper surface of a normal pituitary gland resulting together from a narrow sellar width (a) coronal T1WI and from an unusual thick infe-

rior coronary sinus, demonstrated with dynamic MRI (b–d) (arrow). Normal enhancement of the pituitary gland

Further Reading

Bonneville JF (2002) When the pituitary swells up a little.

J Radiol 83(3):319–320

Cattin F, Bonneville JF, Tang YS (1990) Diagnostic d'une hypophyse convexe. Rev Inst Med 2:221–228

Nonfunctioning Pituitary Macroadenoma: General Points

4

Jean-François Bonneville

Nonfunctioning pituitary macroadenomas, also named nonsecreting adenomas, are frequently in fact gonadotropic adenomas, more rarely null-cell adenomas. They are responsible for neurologic symptoms (mainly visual field defect, headache) or endocrinologic symptoms (mainly anterior pituitary insufficiency). They are also very frequently discovered by chance and can be totally asymptomatic. In the latter case, a conservative approach can be proposed, particularly in the elderly, with a long-term MRI follow up. In young patients, finding a large, invasive pituitary adenoma—secreting or not—should prompt research of AIP and MEN1 gene mutations. Family history of pituitary adenomas or other features of the MEN1 syndrome in the patient and family should also be used to orient genetic research. In every case, a strict imaging protocol must be applied after surgery, the risk of recurrence being around 30 %. Pituitary nonfunctioning macroadenomas are usually centered by an enlarged sella turcica. Signal intensity is usually inhomogeneous, particularly on T2W images with disseminated areas of hyperintensities reflecting cystic or necrotic components. T1 hyperintensity indicates the presence of blood, as does fluid-fluid level (Figs. 4.1 and 4.2). Old hemorrhage may be detected on T2*WI only (Fig. 4.3). Gadolinium injection offers a more clear-cut demonstration of tumoral contours; it enhances the normal pituitary tissue, which is distorted and displaced laterally on one side, and superiorly, but quite never inferiorly (Fig. 4.4). Demonstration of the normal residual pituitary

gland is of crucial importance for the neurosurgeon. Enhancement of the dura, the so-called dural tail (Figs. 4.4 and 4.5), previously described as specific of meningiomas, has been described with large pituitary adenomas, especially if hemorrhagic or soon after surgery, and with perisellar aneurysms and other sellar tumors. The degree of enhancement of the solid part of the pituitary adenoma does not reflect the vascular density of the tumor and is thus not predictable of a potential perioperative hemorrhage. Conversely, flow-void linear images on T1WI or T2WI indicate the presence of intratumoral arteries (Fig. 4.6). Nonfunctioning macroadenomas present usually with an extrasellar extension, upward into the suprasellar cistern, downward into the sphenoid sinus, or laterally into the cavernous sinus. Upward extension is present in more than 70 % of cases. The suprasellar component of the largest macroadenomas is often multilobular (Fig. 4.7). The sellar diaphragm can operate as a belt, giving the adenoma an hourglass shape. If the suprasellar extension is moderate, the T1-hyperintense posterior lobe is compressed and flattened, and best identified in axial T1 fat-saturated noncontrast WI. Aberrant storage of antidiuretic hormone, the so-called ectopic posterior lobe, occurs when the pituitary stalk is severely compressed, i.e., in practice with macroadenomas more than 20 mm in height (see Chap. 53). Various degrees of distortion or thinning of the optic chiasm can be observed. Its hyperintensity on T2WIs could indicate a poor visual prognosis, but the lesion can be